Thrombogenesis and Hemodynamics in Left Atrium Under Atrial Fibrillation

João Lameu[1], Ítalo Sandoval[1], João Salinet[1]

[1] Center for Engineering, Modeling and Applied Social Sciences (CECS), HEart Lab - Biomedical Engineering, Federal University of ABC (UFABC), São Bernardo do Campo, Brazil

Abstract

Atrial fibrillation (AF) is the most common sustained cardiac arrhythmia increasing the risk of stroke in five-fold. Improving knowledge at its development and prevention is crucial for AF patient management. This study aimed to predict the thrombogenesis in left atrium (LA) under AF by a multi-physics approach coupling a 3D transient profile of realistic electrophysiological activity, oscillatory mechanical effects and a biochemical model for thrombogenesis. The local mechanical effects from detailed AF activity disturbed the blood flow pattern, resulting in pro-thrombotic zones in left atrial appendage apex, in contrast with simplified AF model (rigid walls), that could lead to overestimation of pro-thrombotic zones.

1. Introduction

Atrial Fibrillation (AF) is the most common cardiac arrhythmia worldwide, being the main cause of cerebral ischemia, myocardium infarction and venous thromboembolism [1]. About one-third of arrhythmia related hospitalizations are due to AF. AF alters the contraction patterns of atria and could lead to increase in rigidity of atrial walls, consequently, leading to blood stagnation zones and prothrombotic environment, especially in the left atrial appendage (LAA) [2]. In healthy individuals, LAA presents high contractility, preventing blood stasis, in contrast with AF patients with reduced or absent LAA contractility [1].

Computational Fluid Dynamics (CFD) appears as a robust tool, allowing a multi-physics approach coupling electrophysiological and biomechanical aspects and also biochemical modeling of thrombogenesis [3]. Numerical studies of AF considered rigid walls for left atrium (LA) as the worst scenario [4]. Few papers approached the mechanical effects of atrial walls, proposing idealized fibrillation patterns [4, 5] and reporting that more realistic patterns must be considered. Recently, simplified biochemical models have been proposed [3, 6] in order to capture the main characteristics of thrombus formation. Also, artificially accelerated kinetics has been approached to reduce the minimum time to predict the thrombus to a few cardiac flow cycles (about 10-20 cycles, i.e., $\approx$ 4-10 s) [7], in contrast with the real characteristic time of coagulation, about several minutes [6]. Despite these advances, few studies used such an approach in FA studies [3]. Accordingly, this study aimed to predict the thrombogenesis in LA under AF through a multi-physical approach for electrophysiological, biomechanical and biochemical modeling of coagulation cascade.

2. Mathematical Modeling

The integrated model was developed in the CFD code Ansys Fluent (ANSYS, Inc.). AF electrophysiological activity was used as boundary condition for the hemodynamic simulations. Also, a simplified biochemical model was considered to evaluate the thrombogenesis risk.

2.1. AF Electrophysiological Activity

The electrophysiological activity was obtained from LA phantom by simulating a of rotor-type AF [8] using Python. The model (atrial shell) was composed by 284,578 nodes, with a gradient on the properties of it's cells, creating AF propagation patterns, as well as fibrotic tissue, modeled as nodes randomly disconnected [8, 9]. The activation frequency of the signals was firstly obtained by detecting the activation time with the wavelet method [9], then the frequency was calculated by the inverse of the time length between activation. The AF mapping was obtained for 64 points mimicking a multi-electrode array (Fig. 1-a). The AF frequency was re-mapped as a boundary condition in the CFD mesh (Fig. 1-b) to reproduce the local oscillatory mechanical effects into blood flow.

2.2. Governing Equations of Blood Motion

A transient model was proposed, considering incompressible blood flow under laminar regime conditions [4, 5]. A patient-specific LA was taken from an opening dataset [12], being pre-processed in Ansys SpaceClaim (ANSYS, Inc.), and then a volumetric mesh with about 400,000 elements was created in Ansys Meshing (ANSYS,

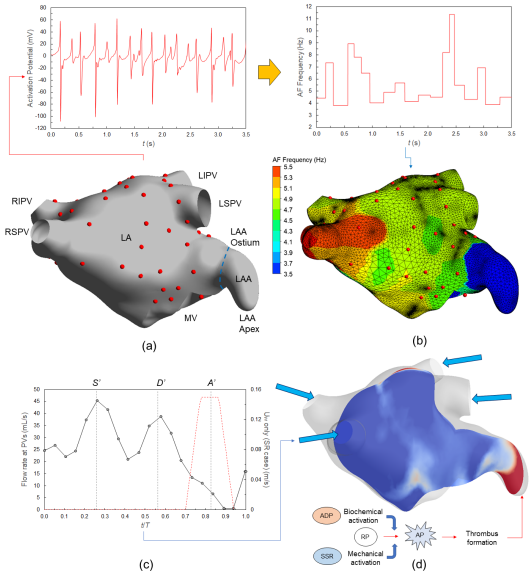

Figure 1. Schematics of integration of AF electrophysiological data in the hemodynamic model: (a) 3D mapping of AF activity from 64-electrode with EGMs; (b) determination of local AF frequency (f_{AF}), providing a 3D transient map of f_{AF} as a boundary condition for the CFD mesh to reproduce the mechanical effects of oscillatory wall motion; (c) definition of inlet flow rates at pulmonary veins (PVs) [10], red dotted lines: LAA wall velocity, prescribed only for SR case [11] and (d) coupling of biochemical model for thrombogenesis (T is the total cardiac flow cycle, LSPV - left superior pulmonary vein, LIPV - left inferior pulmonary vein, RSPV - right superior pulmonary vein, RIPV - right inferior pulmonary vein, LAA - left atrial appendage, AP - activated platelets, RP - resting platelets, ADP - adenosine diphosphate, SSR - shear strain rate).

Inc.). The mass conservation and and momentum balance equations for the blood flow are given by Eq. 1:

$$\nabla \cdot \mathbf{U} = 0 \quad \text{and} \quad \frac{D\mathbf{U}}{Dt} = -\nabla p + \nabla \cdot \quad + \mathbf{f} \qquad (1)$$

where is the specific mass [= 1055 kg m ^{3}], $\mathbf{U}$ is the velocity vector [m s ^{1}], p is the pressure [kg m ^{1}s ^{2}], is the viscous stress tensor [kg m ^{1}s ^{2}] and $\mathbf{f}$ represent the additional momentum source [kg m ^{2}s ^{2}] (Eq. 2). The blood rheology was considered by the Carreau-Yasuda model with rheological parameters from [13].

2.3. Electromechanical Modeling

The mechanical effects of atria wall motion were considered by a momentum-based method, i.e., the atria walls were considered rigid and an additional source was included in the fluid momentum balance ($\mathbf{f}$ in Eq. 1). Basically, an inertial effect induced by the wall motion was considered (Eq. 2). The wall velocity (U_w) was considered to be an isotropic velocity field depending on the electrophysiological phenomenon.

For SR case, the atrial contraction was based on a prescribed velocity function [11] at the end of the cardiac flow cycle (Fig. 1-c, red dotted lines). For AF case using realistic electrophysiological activity, the wall velocity was computed from the oscillatory wall displacement, d_w (Eq. 3), described by a first-order sinusoidal function, with wall displacement amplitude $A = 0.88$ mm (persistent AF) [14] and AF frequency given by the 3D transient profile (Fig. 1-b), is the electrophysiological activity coefficient, used to take into account the propagation effect of wall motion into blood flow.

$$\mathbf{f} = \left(\frac{U_w - \mathbf{U}}{t}\right) \qquad (2)$$

$$U_w = \frac{d_w^{t_i} - d_w^{t_{i-1}}}{t} \quad \text{with} \quad d_w = A \,\text{sen}\,(2 \quad f_{AF}\, t) \qquad (3)$$

$$\frac{@\,'}{@t} + \mathbf{U} \cdot \nabla\,' = \quad _{activ} \qquad (4)$$

where = $_{activ} = 1.0$ for active walls, = $_{activ} = 0$ for non-active walls, = ′ for fluid domain.

2.4. Biochemical Modeling of Thrombogenesis

The simplified biochemical model for thrombogenesis (BMT) proposed by [7] was coupled to the hemodynamic model. The BMT starts from the intrinsic path of coagulation, that can induce thrombus generation in the absence of tissue factor. Two cellular species - resting (RP) and activated platelets (AP) and one biochemical species - adenosine diphosphate (ADP), were considered in the numerical model by advective-diffusive-reactive equations:

$$\frac{@[A_i]}{@t} + \mathbf{U} \cdot \nabla[A_i] = D_{A_1} \nabla^2 [A_i] + S_{A_i} \qquad (5)$$

$$S_{\mathrm{AP}} = -S_{\mathrm{RP}} = \frac{S_{\mathrm{ADP}}}{[\mathrm{ADP}]_r} = k_1 f_1[\mathrm{AP}][\mathrm{RP}] + k_2 f_2[\mathrm{RP}] \qquad (6)$$

where $[A_i]$ is the molar concentration of the i-th species (A_i = AP, RP, ADP) [M], D is the mass diffusion coefficient [m^2 s ^{1}], S is the mass source due to the biochemical reactions [M s ^{1}], given by two contributions: biochemical (f_1) and mechanical (f_2) activation factors, based on thresholds from experimental data [7]. $[\mathrm{ADP}]_r$ is the relative ADP released from dense granules, k_1 and k_2 are the accelerated kinetic constants for biochemical and mechanical activation. The model parameters were:

$k_1 = 3 \cdot 10^8$ [$M^{-1} s^{-1}$], $k_2 = 0.6$ [s^{-1}], $D_{AP} = D_{RP} = 10^{-11}$[$m^2 s^{-1}$], $D_{ADP} = 2.57 \cdot 10^{-10}$[$m^2 s^{-1}$], $[ADP]_r = 562.5$ (release of 75% of ADP content) [7]. Details of f_1 and f_2 are found in [7].

2.5. Study Cases and Thrombogenesis Indicators

Three study cases were performed with Carreau-Yasuda (CY) rheological model: SR-CY: sinus rhythm, AF-CY: simplified AF case (rigid walls), AF-CY-3D-EGM: AF case with realistic 3D electrophysiological activity at LA walls. For the SR case, the cardiac flow cycle length was considered T = 940 ms (i.e. 64 bpm) [10], while for AF cases T = 462 ms (i.e. 130 bpm). 5 s of cardiac flow was simulated with time-step of $1 \cdot 10^{-3}$ s and a root mean square (RMS) residual of $1 \cdot 10^{-4}$. The inlet boundary condition was considered as the prescribed pulsatile flow (Fig. 1-c), considering a flow rate symmetry among the PVs [2]. The outlet condition (mitral valve), was considered as a fixed open area with constant pressure of 8 mmHg [2]. The LA walls were considered rigid and the momentum-based method (described in Section 2.3), reproduced the oscillatory wall motion in AF cases, while a prescribed LAA wall velocity [11] was considered to reproduce the atrial contractility only for SR case. The boundary conditions for the BMT model were: [RP] = 10 [nM], [AP] = 0.5 [nM] (i.e., 5% of AP), [ADP] = 250 [nM].

Pro-thrombotic zones were estimated from wall shear stress indicators and thrombus aggregation intensity (, Eq. 7). TAWSS is the time-averaged $_w$ along the total cardiac cycle time T, OSI is the oscillatory shear index, ranging from 0 to 0.5 (0.5 indicates a strong recirculation zones) and RRT is the local relative residence time in [Pa]$^{-1}$. Higher values of OSI and RRT and lower values of TAWSS indicate pro-thrombotic zones:

$$\frac{@}{@t} = \quad P_{TSP} \; ^{2}_{f} - \tag{7}$$

where and are empirical constants for accumulation and destruction of thrombi [6], obtained from *in vitro* data in a Backward Facing Step (BFS) benchmark, P_{TSP} is the thrombus susceptibility potential, ranging from 0 to 1 as a function of WSS thresholds, $_f$ is the fraction of activated platelets [6]. The stable thrombi generation is related to a threshold for . Since the BMT model employs accelerated kinetics, the threshold needed to be estimated considering the parameters from [7] and the proposed threshold ($_{BFS}$) from [6]. Thus: $_{threshold} \approx {}_{BFS}(k_{kin;BQ} \cdot k_{kin;mech} \cdot t_{kin})/(k_{BFS;BQ} \cdot k_{BFS;mech} \cdot t_{BFS}) \approx 10^{-12} \cdot (10^8 \cdot 10^{-1} \cdot 10^1)/(1 \cdot 1 \cdot 10^3) \approx 10^{-7}$[cm^{-3}], where the subscripts BQ and $mech$ denote for the magnitude of biochemical and mechanical kinetic constants, t is the timescale of stable clot formation, kin and BFS denotes for accelerated kinetics from [7] and data from [6], respectively.

3. Results and Discussion

Fig. 2 presents the time-averaged fields of WSS indicators (TAWSS, OSI, RRT) and instantaneous fields at the end of cardiac flow cycle (instant A^0, Fig. 1-c) for SSR, velocity vectors and . From Fig. 2-a,b, it was observed low values of TAWSS (< 0.1 [Pa]) in the LAA under AF conditions. The AF-CY predicted stagnation zones in the whole LAA, with SSR < 10 s^{-1}, as observed in Fig. 2-e. The AF-CY-3D-EGM model predicted higher values of TAWSS, due to the local flow perturbation inherent from the oscillatory effect of AF activity. This mechanical effect propagates inwards the whole LA, including the LAA zone, where it was noticed higher values of TAWSS (Fig. 2-b) and SSR (Fig. 2-e), inherent from a slightly acceleration of blood flow (Fig. 2-f) regarding the AF-CY (rigid wall) model. The consideration of the atrial contraction by the momentum method in the SR model provided local acceleration of blood (Fig. 2-f) increasing the TAWSS (Fig. 2-a) and reducing the blood stagnation, as expected for healthy conditions. The OSI field shows (Fig. 2-c) higher recirculation zones in the middle section of the LA (between left and right PVs) and also in LAA under AF conditions. The AF-CY-3D-EGM model predicted zones with higher OSI near to LAA ostium where the blood fluid accelerated (Fig. 2-f) due to the oscillatory perturbation from LA walls under AF. Consequently, larger RRT were observed in LAA (Fig 2-d) for AF cases. The results agree with the expected hemodynamics with stagnation zones inside the LAA under AF, resulting in a pro-thrombotic environment.

Fig. 2-f shows the velocity vector fields at instant A (atrial contraction), where it can be observed the local acceleration of the blood from LAA, reproducing its contractility under healthy conditions. The zones of low velocity (< 0.05 m/s) are related to low strain rates and consequently higher apparent viscosities. The LAA contractility observed in SR case, results in higher strain rates (Fig. 2-e) due to the local acceleration of blood, in contrast with the strain rates < 10 s^{-1} in LAA from AF-condition, which is directly related to rouleaux formation and increment of blood apparent viscosity. The hemodynamic patterns directly affect the biochemical behavior of thrombogenesis. Fig. 2-g shows the aggregation intensity field after 4.5 s of simulation. As expected from the WSS-based indicators, higher values of , above the $_{threshold}$ were observed in the pro-thrombotic zone of LAA under AF conditions. The AF-CY model provided a larger zone above $_{threshold}$ inherent from the strong stagnation zone over the whole LAA, while the AF-CY-3D-EGM model resulted in prediction of thrombi growth only at LAA apex.